Supporting Information: "Inducing Stratification of Colloidal Mixtures with a Mixed Binary Solvent"

Binghan Liu,[1] Gary S. Grest,[2] and Shengfeng Cheng[3,*]

[1] *Department of Physics, Center for Soft Matter and Biological Physics, and Macromolecules Innovation Institute, Virginia Tech, Blacksburg, Virginia 24061, USA*

[2] *Sandia National Laboratories, Albuquerque, NM 87185, USA*

[3] *Department of Physics, Center for Soft Matter and Biological Physics, Macromolecules Innovation Institute, and Department of Mechanical Engineering, Virginia Tech, Blacksburg, Virginia 24061, USA*

(Dated: October 31, 2023)

Here we include results on the receding speed of the liquid-vapor interface during evaporation and a direct comparison of the nanoparticle concentration profiles along the z-axis under the various evaporation schemes discussed in the main text.

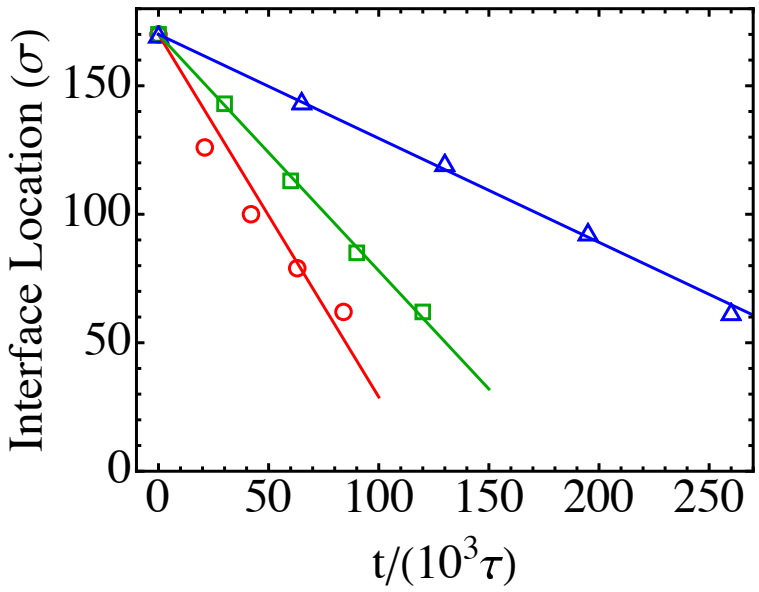

FIG. S1. Location of the receding liquid-vapor interface vs. time under various solvent evaporation schemes: evaporating into a vacuum (red circles), evaporating at a fixed intermediate rate of j_p (the terminal plateau rate of the evaporating-into-vacuum scheme, green squares), and evaporating at a fixed rate of $j_s \simeq j_p/3$ (blue triangles). The lines are linear fits whose slopes yield the receding speed of the interface, v_e.

The location of the liquid-vapor interface during solvent evaporation is plotted against time in Fig. S1. At a fixed evaporation rate, the liquid-vapor interface recedes almost uniformly at a constant speed, v_e. Under the evaporating-into-vacuum scheme, the interface location varies with time nonlinearly and the rate of change decreases as time proceeds. This reflects the fact that when the solvent vapor escapes into a vacuum, the evaporation rate is initially high, then decreases with time, and eventually levels off in the long time limit. For each data set included in Fig. S1, a linear fit is performed to determine v_e. For the evaporating-into-vacuum scheme, $v_e \simeq 1.4 \times 10^{-3}\sigma/\tau$. At the intermediate solvent evaporation rate, $v_e \simeq 0.92 \times 10^{-3}\sigma/\tau$ and at the slow rate, $v_e \simeq 0.40 \times 10^{-3}\sigma/\tau$.

The concentration profiles of α and β nanoparticles in the drying film of a thickness of about 62σ are compared directly in Fig. S2. Under the slow evaporation rate, the two types of nanoparticles phase separate more strongly and the middle α-layer is thicker. The

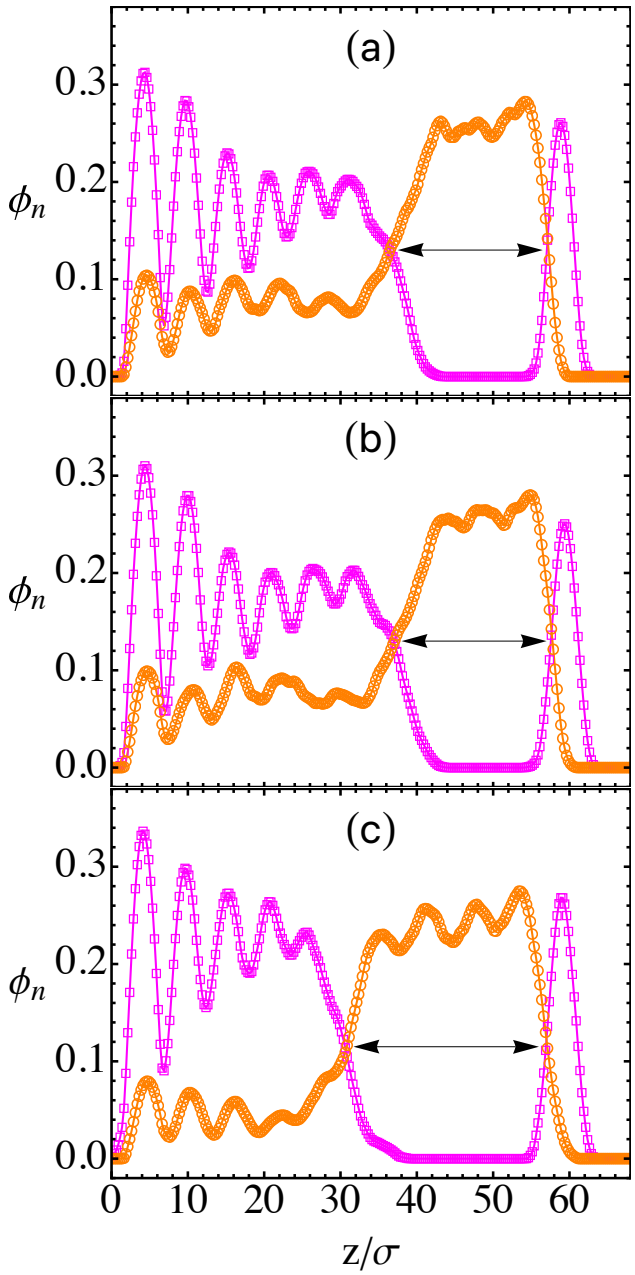

FIG. S2. Concentration profiles of the two types of nanoparticles (α in orange and β in purple) in the drying film at a thickness of $\sim 62\sigma$ under the three solvent evaporation schemes: (a) evaporating-into-vacuum, (b) fixed intermediate rate, and (c) fixed slow rate. The arrows indicate the width of the middle α-layer.

concentration of α nanoparticles in the bottom β-layer is also smaller in this case than under the other two evaporation schemes.

To quantify the thickness of the middle α-layer, we identify the crossing points in the

concentration profiles, as indicated by the arrows in Fig. S2. The thickness is computed as the difference of the two crossing points, on the two sides of the α-layer, along the z-axis. It is about 21σ for the evaporating-into-vacuum and intermediate-rate schemes and about 26σ for the slow-rate scheme.

Two sample input scripts for LAMMPS runs are provided: "in.binary_equi_150.txt" and "in.binary_fix_fast_150.txt".

---

* chengsf@vt.edu